

Performance Improvement of Grid-Connected DFIG-Based Wind Turbines with an ANFIS-Based LVRT Controller

Dr. D. Obulesu

¹Associate Professor, Department of EEE, CVR College of Engineering, Telangana, Hyderabad, India.

Dr. K. Shashidhar Reddy

²Professor, Department of EEE, CVR College of Engineering, Telangana, Hyderabad, India.

Abstract - In this paper, a comparative analysis of fuzzy-based and adaptive neuro-fuzzy inference system (ANFIS)-based low-voltage ride-through (LVRT) of a wind turbine based on a grid-connected doubly fed induction generator (DFIG) is performed. The turbine's transient characteristics are studied in depth, and the dynamic behaviour of DFIGs during both asymmetrical and symmetrical grid voltage sags are thoroughly investigated. The results obtained in this study provide clear evidence that the proposed ANFIS method proves more effective compared with the LVRT-based fuzzy controller.

Index Terms - Doubly fed induction generator, low-voltage ride-through (LVRT), LVRT-based fuzzy controller, ANFIS-based low-voltage ride-through.

1. INTRODUCTION

There have been significant developments in clean and sustainable electricity generation from renewable resources in the last few decades. Despite there being great potential for the usage of alternative energy conversion systems in various autonomous and grid-connected applications, certain drawbacks, such as intermittent and seasonal variability of primary resources, have severely limited the access of these clean energy systems in the power generation market [1–2].

An innovative controllable crowbar based on the fault-type protection technique for a doubly fed induction generator (DFIG) wind energy conversion system connected to a grid was proposed by Omar Nourelddeen et al. [3,9]. This system, each with a capacity of 1.5 MW, is constituted of six DFIG wind turbines. The operational method involves connecting a set of crowbar resistors using different connection mechanisms by activating the controllable circuit breakers (CBs) depending on the detected fault type. Each phase of DFIG had a crowbar resistor connected in parallel with a controllable CB, with all finally being connected in series to grid terminals. The adaptive neuro-fuzzy inference system (ANFIS) networks can provide functionalities like detecting fault occurrence, categorizing the fault types, activating CBs for crowbar resistors associated with faulted phases during the fault period, and deactivating them after fault clearance.

Some other studies by R.P.S. Leao, Dakka Obulesu et al. [4,10] assessed the operation of the low-voltage ride-through (LVRT) curve in two numerical relays from different manufacturers besides analysing the features of both the relays and the obtained LVRT curve. Those studies also examined the functionality of wind turbine grid protection systems in a simplified power system by means of the PSCAD/EMTDC simulation tool.

Y. Tsukamoto et al. [5–8] estimated ANFIS parameters to allow characterization of both the Sugeno and Tsukamoto fuzzy models using the ANFIS architecture. Here, the fuzzy logic considered the imprecision and uncertainty of the system being modelled and the required adaptability was provided by the neural network. The hybrid method developed in the work involved deriving an initial fuzzy model along with its input variables using the rules resulting from the input–output data of the system being modelled. This was followed by fine-tuning the rules of the initial fuzzy model using the neural network to construct the final ANFIS model of the system. As previously, ANFIS was used as the basis to establish real-world systems here too.

II.SIMULINK MODEL

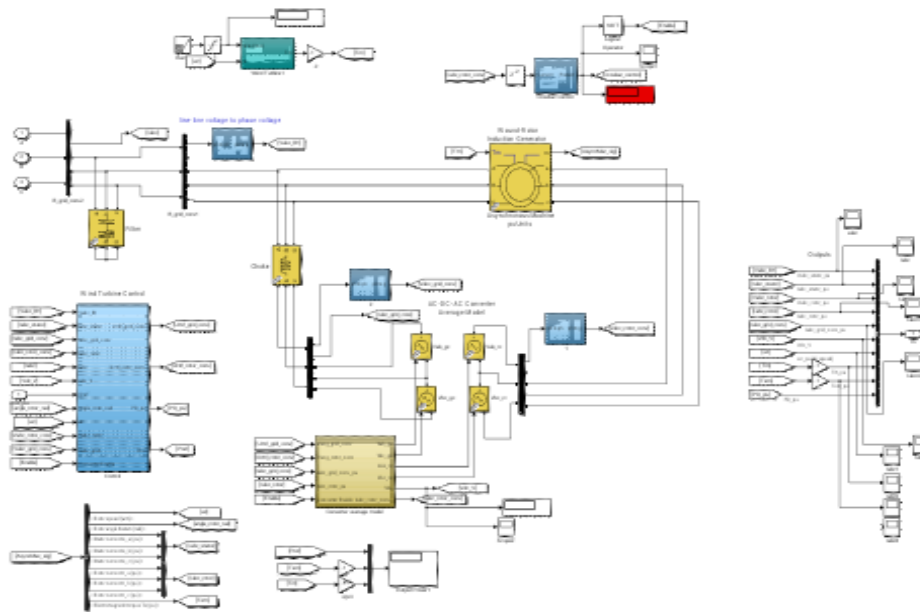


Fig. 1. Simulation diagram of the test system

Fig.1 depicts the simulation diagram of the test system with both the ANFIS-based and fuzzy-based LVRT controllers. Fig. 2 provides a detailed depiction of the internal structure of the DFIG. The membership functions of input 1 and input 2 are shown in Fig. 3 and Fig. 4, respectively. The output membership functions are displayed in Fig. 5. All input and output membership functions can be classified into seven membership functions, namely, NL, NM, NS, Z, PS, PM, and PL. Barring NL and PL, all other membership functions are considered triangular, with the remaining being trapezoidal. Fig.6 and Fig 7 show the fuzzy-logic-based LVRT controller rule viewer and the fuzzy-logic-based LVRT controller rule viewer surface, respectively.

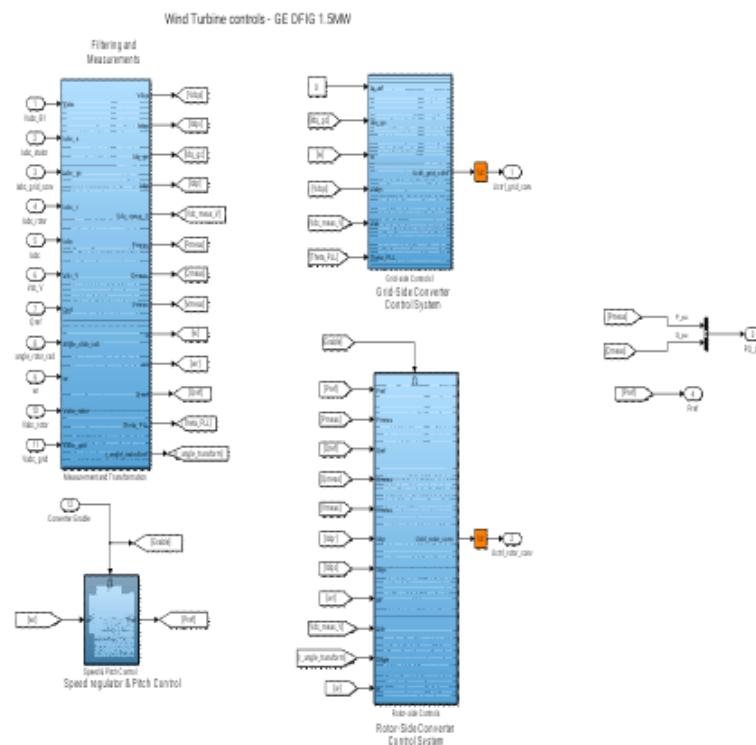


Fig. 2. Internal structure of the DFIG

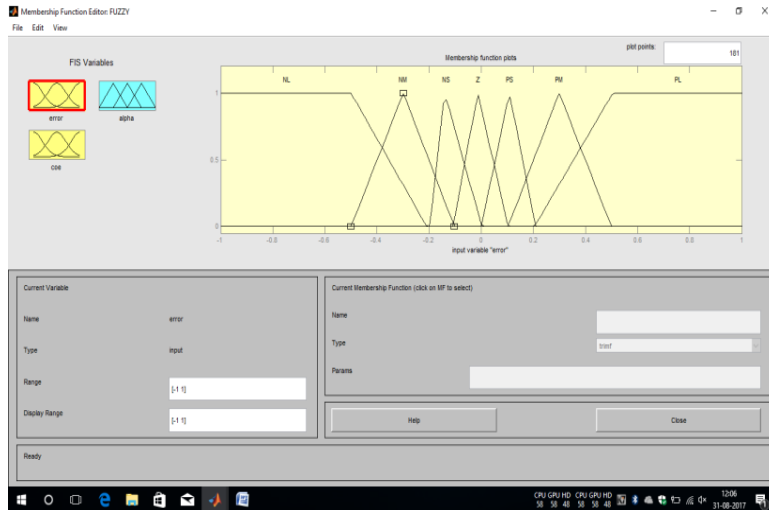


Fig. 3 Fuzzy-logic-based LVRT controller error membership functions.

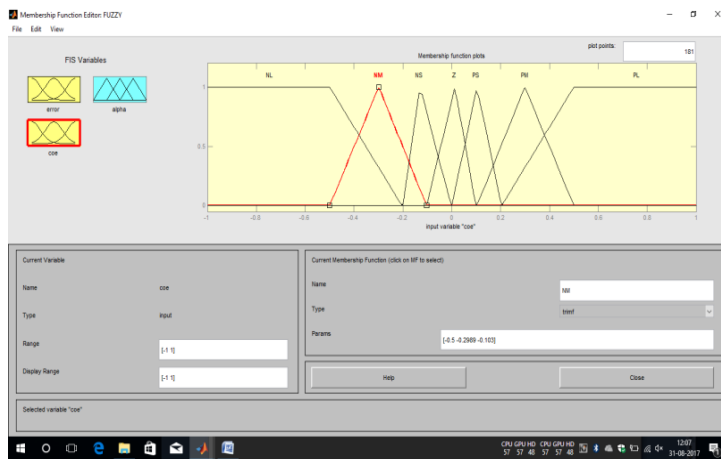


Fig. 4 Fuzzy-logic-based LVRT controller change in error membership functions

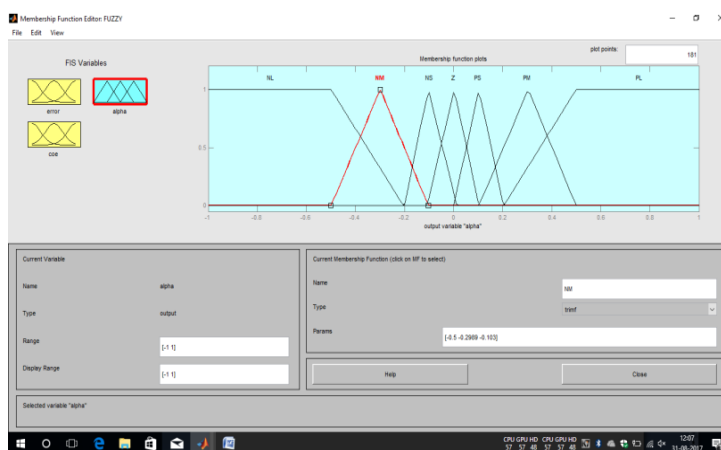


Fig. 5 Fuzzy-logic-based LVRT controller output membership functions

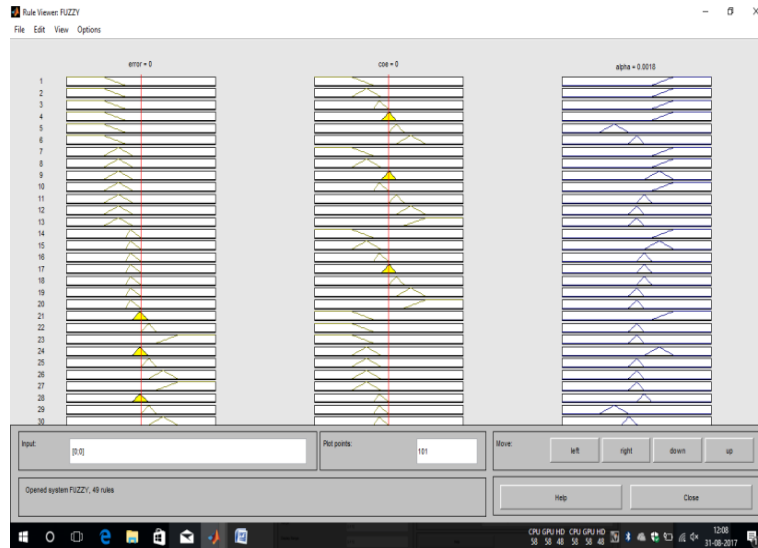


Fig. 6 Fuzzy-logic-based LVRT controller rule viewer

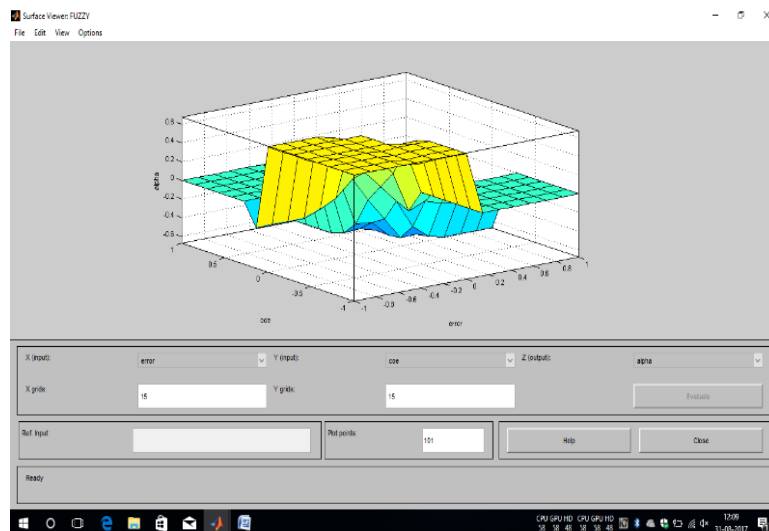


Fig. 7 Fuzzy-logic-based LVRT controller rule viewer surface

III. DFIG MODEL

The DFIG, often used in wind turbines, is an adaptable speed induction machine. [3]

$$u_{ds} = R_s i_{ds} - \omega_s \varphi_{qs} + \frac{d\varphi_{ds}}{dt} \quad -- (1)$$

$$u_{qs} = R_s i_{qs} + \omega_s \varphi_{ds} + \frac{d\varphi_{qs}}{dt} \quad --(2)$$

$$u_{dr} = R_r i_{dr} - \omega_r \varphi_{qr} + \frac{d\varphi_{dr}}{dt} \quad --(3)$$

$$u_{qr} = R_r i_{qr} + \omega_r \varphi_{dr} + \frac{d\varphi_{qr}}{dt} \quad --(4)$$

Here,

$u_{ds}, u_{qs}, u_{dr}, u_{qr}, i_{ds}, i_{qs}, i_{dr}, i_{qr}, \varphi_{ds}, \varphi_{qs}, \varphi_{dr},$ and φ_{qr}

denote the d-q components of stator and rotor voltage currents and fluxes linkages, R_s denotes the resistance of the stator, R_r denotes the resistance of rotor windings, ω_s denotes the angular frequency of the stator current, and ω_r denotes the angular frequency of the rotor current. The equations below express the total active power and reactive power for both stator and rotor sides respectively [3]:

$$P = P_s + P_r \quad --(5)$$

$$Q = Q_s + Q_r \quad --(6)$$

In equation 5, P denotes the total active power, P_s denotes the stator active power, and P_r denotes the rotor active power. In equation 6, Q denotes the total reactive power, Q_s denotes the stator reactive power, and Q_r denotes the rotor reactive power.

IV. RESULTS AND DISCUSSION

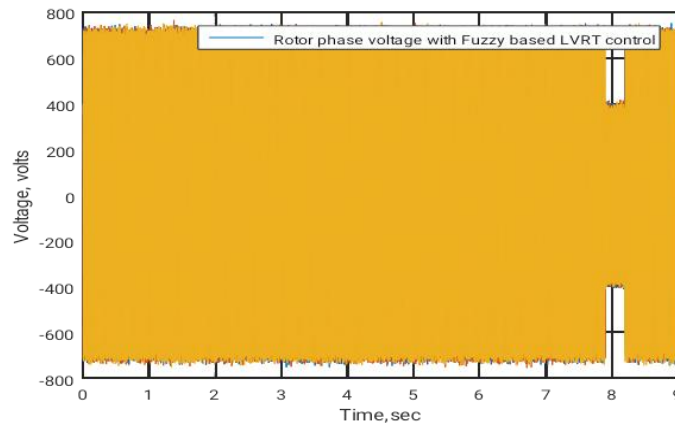


Fig.8 Rotor phase voltage with Fuzzy-logic-based LVRT controller

Fig. 8 depicts the rotor phase voltage of DFIG with the fuzzy-logic-based LVRT controller. The fault is created and cleared at 7.9 seconds and 8.21 seconds respectively, which testifies to the effectiveness of this controller. Falling to 380V during the fault period, the voltage of the rotor reaches 720V after clearing.

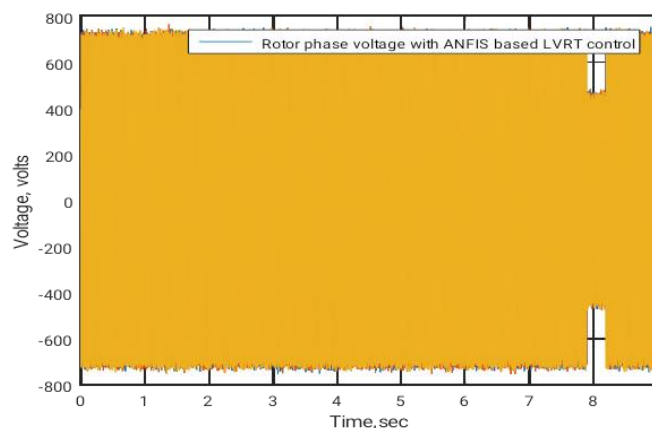


Fig.9 Rotor phase voltage with the ANFIS-based LVRT controller.

Fig. 9 depicts the rotor phase voltage of DFIG with the ANFIS-based LVRT controller. The fault is created and cleared at 7.9 and 8.21 seconds respectively, which testifies to the effectiveness of this controller. Falling to 450V during the fault period, the voltage of the rotor reaches 720V after clearing. The proposed controller showed an increase of 70V during the fault when compared to the fuzzy-logic-based LVRT controller. From the perspective of rotor voltage, the proposed controller proves to be more effective than the fuzzy-logic-based LVRT controller.

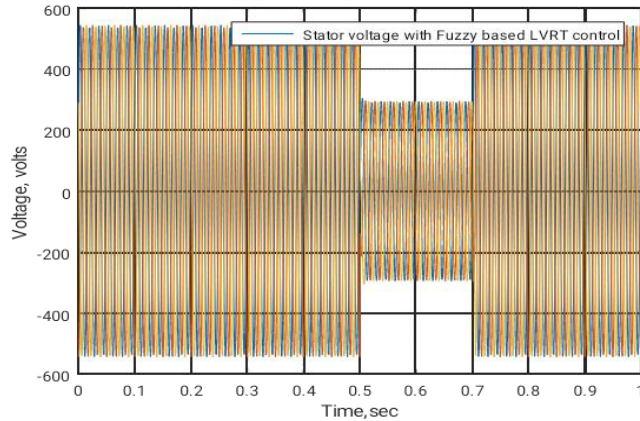


Fig.10 Stator phase voltage with the fuzzy-logic-based LVRT controller.

Fig. 10 depicts the stator phase voltage of DFIG with the fuzzy-logic-based LVRT controller. The fault is created and cleared at 7.9 and 8.21 seconds respectively, which testifies to the effectiveness of this controller. Falling to 280V during the fault period, the voltage of the rotor reaches 500V after clearing. Fig. 11 depicts the stator phase voltage of DFIG with the ANFIS-based LVRT controller. The fault is created and cleared at 0.5 and 0.7 seconds respectively, which testifies to the effectiveness of this controller. Falling to 320V during the fault period, the voltage of the rotor reaches 500V after clearing. Therefore, an enhancement of 40 V presents itself for the proposed controller during the fault when compared with the fuzzy-logic-based LVRT controller. The proposed controller is more effective, from the perspective of stator voltage, than the fuzzy-logic-based LVRT controller.

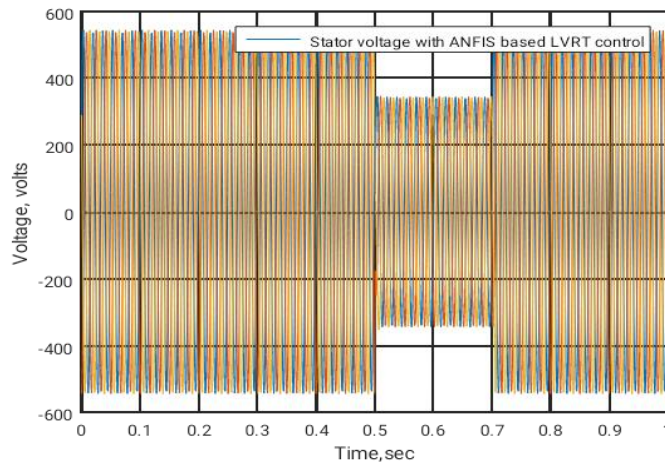


Fig.11 Stator phase voltage with the ANFIS-based LVRT controller.

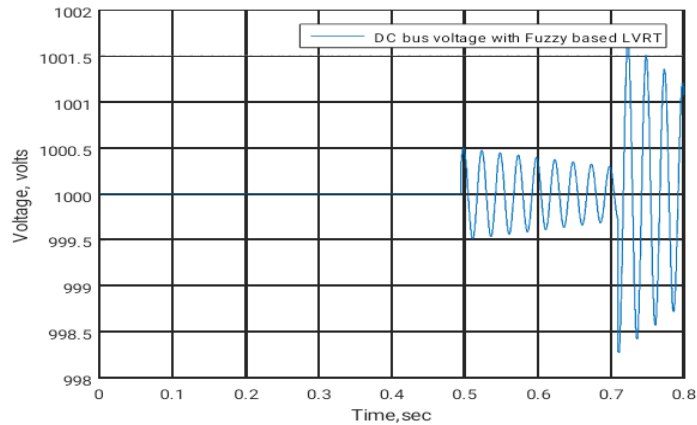


Fig.12 DC bus voltage with the fuzzy-logic-based LVRT controller.

Fig. 12 depicts the DC bus voltage of DFIG with the fuzzy-logic-based LVRT controller. The fault is created and cleared at 0.5 and 0.7 seconds respectively, which testifies to the effectiveness of this controller. Oscillating between 1000.5 and 999.5 V during the fault period, the voltage of the DC bus oscillates between 1000.3 and 999.3 V after clearing.

The DC bus voltage of DFIG with the ANFIS-based LVRT controller is presented in fig.13. The fault is created at and cleared 0.5 and 0.7 seconds respectively, which testifies to the effectiveness of this controller. Oscillating between 1001.5 and 999.5 V during the fault period, the voltage of the DC bus oscillates between 1000.2 and 999.2 V, after clearing.

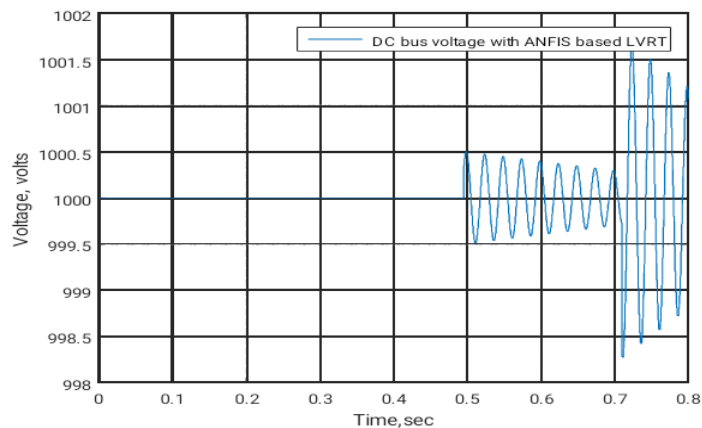


Fig.13 DC bus voltage with the ANFIS-based LVRT controller

The rotor phase current, the stator phase voltage, and the DC bus voltage with the fuzzy-logic-based LVRT controllers are compared with the ANFIS-based LVRT controllers. It can be stated from the simulation results that the proposed controller provides better voltage and current support as compared with the fuzzy-logic-based LVRT controller.

IV. CONCLUSION

A comparison of the rotor phase current, the stator phase voltage, and the DC bus voltage with the fuzzy-logic-based LVRT controllers is performed with the ANFIS-based LVRT controllers. It can be stated from the simulation results that the proposed controller provides better voltage and current support as compared with the fuzzy-logic-based LVRT controller, hence proving that the proposed ANFIS method is more effective than the LVRT and fuzzy controllers.

REFERENCES

- [1] Herna'n De Battistaa,Ricardo Julia'n et al., "Power conditioning for a wind-hydrogen energy system",22 June 2005, pp.478-486.
- [2] R. Dell, D. R, and Energy storage: a key technology for global energy sustainability, J. Power Sources 100 (1) (2001), pp. 2-17.
- [3] Omar Noureldeen and I. Hamdan "A novel controllable crowbar based on fault type protection technique for DFIG wind energy conversion system using adaptive neuro-fuzzy inference system", Protection and Control of Modern Power Systems,35(2018), pp.1-12.
- [4] R.P.S. Leao, J.B. Almada, P.A. Souza, 'The Implementation of the Low Voltage Ride-Through Curve on the Protection System of a Wind Power Plant', International Conference on Renewable Energies and Power Quality (Spain), 13-15th April 2011
- [5] Y. Tsukamoto, M. M. Gupta, R. K. Ragade, and R. R. Yager, "An approach to fuzzy reasoning method" in Advances in Fuzzy Set Theory and Application, 1979, pp. 137-149.
- [6] J.S.R. Jang and C.T. Sun, "Functional equivalence between radial basis function networks and fuzzy inference systems," IEEE Trans. on Neural Netw., vol. 4, no. 1, pp. 156-159, January 1993.
- [7] A. Pinkus, "Approximation theory of the MLP in neural networks," ACTA Numerical, vol. 8, pp.143-196, 1999.
- [8] J. S. R. Jang and C. T. Sun, "Neuro-fuzzy modeling and control," Proc. IEEE, vol. 83, no. 3, pp.378-406, March 1995 .
- [9] Manohar et al., "A DFIG-based wind energy conversion system(WECS)for LVRT enhancement using a hybrid approach:an efficient MEHRFA Technique, soft computing 25(4),pp.2559-2574,Feb 2021.
- [10] Dr.Dakka Obulesu et al., "Performance Improvement of Grid-Connected DFIG-Based Wind Turbine with a Fuzzy-Based LVRT Controller", Turkish Journal of Computer and Mathematics Education,Vol.12, No.6(2021),3599-3605